bioRxiv preprint doi: https://doi.org/10.1101/2024.03.25.585721; this version posted March 28, 2024. The copyright holder for this preprint (which was not certified by peer review) is the author/funder, who has granted bioRxiv a license to display the preprint in perpetuity. It is made available under aCC-BY-NC-ND 4.0 International license.

Targeting protein-ligand neosurfaces using a generalizable deep learning approach

Anthony Marchand[1]#, Stephen Buckley[1]#, Arne Schneuing[1]#, Martin Pacesa[1], Pablo Gainza[1]†, Evgenia Elizarova[1], Rebecca M. Neeser[1,2], Pao-Wan Lee[3], Luc Reymond[4], Maddalena Elia[1], Leo Scheller[1], Sandrine Georgeon[1], Joseph Schmidt[1], Philippe Schwaller[2], Sebastian J. Maerkl[3], Michael Bronstein[5] & Bruno E. Correia[1]*

[1] Laboratory of protein design and immunoengineering, Institute of Bioengineering, Ecole polytechnique fédérale de Lausanne; Lausanne, CH-1015, Switzerland.
[2] Laboratory of chemical artificial intelligence, Institute of Chemical Sciences and Engineering, Ecole polytechnique fédérale de Lausanne; Lausanne, CH-1015, Switzerland.
[3] Laboratory of biological network characterization, Institute of Bioengineering, Ecole polytechnique fédérale de Lausanne; Lausanne, CH-1015, Switzerland.
[4] Biomolecular screening core facility, School of Life Sciences, Ecole polytechnique fédérale de Lausanne; Lausanne, CH-1015, Switzerland.
[5] Department of Computer Science, University of Oxford; Oxford, OX1 3QD, United Kingdom

* Corresponding author. E-mail : bruno.correia@epfl.ch
# These authors contributed equally to this work
† Present address: Monte Rosa Therapeutics

Abstract

Molecular recognition events between proteins drive biological processes in living systems. However, higher levels of mechanistic regulation have emerged, where protein-protein interactions are conditioned to small molecules. Here, we present a computational strategy for the design of proteins that target neosurfaces, i.e. surfaces arising from protein-ligand complexes. To do so, we leveraged a deep learning approach based on learned molecular surface representations and experimentally validated binders against three drug-bound protein complexes. Remarkably, surface fingerprints trained only on proteins can be applied to neosurfaces emerging from small molecules, serving as a powerful demonstration of generalizability that is uncommon in deep learning approaches. The designed chemically-induced protein interactions hold the potential to expand the sensing repertoire and the assembly of new synthetic pathways in engineered cells.

bioRxiv preprint doi: https://doi.org/10.1101/2024.03.25.585721; this version posted March 28, 2024. The copyright holder for this preprint (which was not certified by peer review) is the author/funder, who has granted bioRxiv a license to display the preprint in perpetuity. It is made available under aCC-BY-NC-ND 4.0 International license.

Main

Protein-protein interactions (PPIs) play an essential role in healthy cell homeostasis, but are also involved in numerous diseases(*1*, *2*). For this reason, several therapies targeting PPIs have been developed over the last decades and multiple computational tools have been recently proposed to design novel protein interactions(*3*). The governing principles determining the propensity of proteins to form interactions are intricate due to the interplay of several contributions, such as geometric and chemical complementarity, dynamics, and solvent interactions. Therefore it remains challenging to predict and design novel PPIs, especially in the absence of evolutionary constraints. Native PPIs can also be controlled by additional regulatory layers such as allostery(*4*), post-translational modifications(*5*), or direct ligand binding(*6*, *7*). Compound-bound surfaces, which we refer to as neosurfaces, are one of the most fascinating and challenging types of molecular recognition instances, where relatively minor changes at the protein binding site can have a large impact on binding affinities. The interest in such interactions has been fueled by the development of new drug modalities; specifically molecular glues that form neosurfaces to trigger protein interactions for degradation and other applications(*8*, *9*), thus representing a promising route for the development of innovative therapeutics.

In synthetic biology, molecular components that rely on small molecule-induced neosurfaces have been used to engineer chemically-responsive systems with precise spatio-temporal control of cellular activities(*10*). Small molecule triggers have been used to both induce and disrupt PPIs, thereby functioning as ON or OFF switches for engineered cellular functions(*10*–*12*). There are several practical advantages in using small molecules as triggers due to their simple administration, biodistribution, cell permeability, safety, and high affinity and specificity to their target proteins. Protein-based switches controlled by small molecules have already been applied to regulate transcription(*13*, *14*), protein degradation(*15*–*17*), and protein localization(*18*–*20*), among many other applications. In addition to their use in basic research, engineering molecular switches is becoming a more common mechanism of controlling protein-based and cellular therapeutics, whose activity may have to be regulated to mitigate potentially dangerous side effects(*11*, *21*, *22*). While several chemically-disruptable heterodimer (OFF-switch) systems have been proposed(*10*, *11*, *21*), computationally designed chemically-induced dimerization (CID, ON-switch) systems remain challenging due to the complexity of modeling neosurfaces. Previous attempts at designing CID systems primarily relied on experimental methods(*10*, *13*, *23*, *24*) and, despite the emergence of artificial intelligence and numerous computational tools, only few tools can generalize to both proteins and small molecules as a target for protein design, resulting in a lack of suitable

bioRxiv preprint doi: https://doi.org/10.1101/2024.03.25.585721; this version posted March 28, 2024. The copyright holder for this preprint (which was not certified by peer review) is the author/funder, who has granted bioRxiv a license to display the preprint in perpetuity. It is made available under aCC-BY-NC-ND 4.0 International license.

approaches for the design of novel chemically-induced PPIs. Computational methods to design novel CIDs mostly relied on transplanting an existing drug binding site to a known heterodimer interface(*25*) or using docking of putative pre-existing proteins (i.e. scaffolds) followed by interface optimization(*26*). However, these approaches can face limitations such as the risk of drug-independent dimerization, the lack of suitable scaffold proteins for design, or the extensive need for *in vitro* maturation techniques.

We recently reported a geometric deep learning-based framework called MaSIF (Molecular Surface Interaction Fingerprinting)(*27*) for the study of protein surface features, and for the design of novel protein-protein interactions(*28*). In this study, we aim to test whether our surface-centric approach can generalize to non-protein ligands without additional training data by using a higher-level representation, namely the geometric and chemical features found on the molecular surface. To do so, we designed site-specific binders that target neosurfaces composed of a small molecule ligand and protein surface moieties, resulting in *de novo* ligand-dependent protein interactions. We successfully designed and characterized novel protein binders recognizing the B-cell lymphoma 2 (Bcl2) protein in complex with the clinically-approved inhibitor Venetoclax(*29*), the progesterone-binding antibody DB3 in complex with its ligand(*30*), and finally the peptide deformylase 1 (PDF1) protein from *Pseudomonas aeruginosa* in complex with the antibiotic Actinonin(*31*). Lastly, we show that such ligand-controlled systems can be utilized in both *in vitro* and cellular contexts for a range of synthetic biology applications, unlocking possibilities for the development and regulation of novel therapeutic approaches.

MaSIF captures interaction propensities of neosurfaces

Within our geometric deep learning framework, MaSIF(*27*), we previously developed two applications: i) *MaSIF-site* to accurately predict regions of the protein surface with a high propensity to form an interface with another protein and, ii) *MaSIF-search* to rapidly find and dock protein partners based on complementary surface patches. In *MaSIF-search*, we extract surface patch descriptors (“fingerprints”), so that patches with complementary geometry and chemistry have similar fingerprints, whereas non-interacting patches have low fingerprint similarity. Surface fingerprints allow to perform an initial ultra-fast search in an alignment-free manner using the Euclidean distances between them. Patches with fingerprint distances below a threshold are then further aligned in 3D and scored with an interface-post alignment (IPA) score to refine the selection.

bioRxiv preprint doi: https://doi.org/10.1101/2024.03.25.585721; this version posted March 28, 2024. The copyright holder for this preprint (which was not certified by peer review) is the author/funder, who has granted bioRxiv a license to display the preprint in perpetuity. It is made available under aCC-BY-NC-ND 4.0 International license.

In its initial conception, MaSIF only considered canonical amino acids as part of the protein molecular surface and was not compatible with small molecules, glycans, and other ligands. Thus, we present here *MaSIF-neosurf* to incorporate small molecules as part of the molecular surface representation of the target protein to predict interfaces and partners based on the neosurface fingerprints (Fig. 1A, see Methods). MaSIF was initially trained to operate on general chemical and geometric surface properties of biomolecules, while abstracting the underlying structure. Thus, it is not restricted to only protein surfaces, but should in principle also capture the surface patterns arising from other non-protein surfaces. Upon generation of the molecular surface of the protein-drug complex, *MaSIF-neosurf* computes the two geometric features: shape index(*32*) and distance-dependent curvature(*33*). In addition, three chemical features are also used: Poisson-Boltzmann electrostatics, which can be computed directly from the small molecule, and hydrogen bond donor/acceptor propensity(*34*) and hydrophobicity(*35*–*37*), for which we developed new featurizers tailored to capture the chemical properties of the small molecules (see Methods and fig. S1).

To assess the capabilities of *MaSIF-neosurf*, we benchmarked its performance on several ternary complexes whose interface is composed of protein and ligand surfaces. We aimed to recover known binding partners for proteins with small molecules at the binding interface. After assembling a list of 14 ligand-induced protein complexes, we split each of them into two subunits, resulting in 28 independent benchmarking cases, and processed them with and without the small molecule bound. The ligand-free protein surfaces, together with 200 decoy proteins, constitute our database, which we query with surface patches from all 28 protein-ligand complexes. Since each of the 228 protein candidates is decomposed into almost 4000 patches on average, the database represents a large search space with more than 900’000 potential binding sites. We then evaluated whether the correct binding partner is retrieved and docked in the correct rigid-body orientation. When considering the protein-ligand complex as a docking partner, *MaSIF-neosurf* recovers more than 70% of the correct binding partners and their binding poses (Fig. 1B). Only a small subset of test cases could be recovered in the absence of the ligand and the general trend is that in such cases the protein surface is a large contributor towards the overall protein interaction (fig. S2). The ability to capture the neosurface properties is further supported by an increased descriptor distance score between interacting partners (i.e. an increased complementarity between interacting fingerprints, see Methods) and an increased interface post-alignment (IPA, see Methods) score in the presence of the small molecule compared to the case without (Fig. 1C-D). Overall, *MaSIF-neosurf* captures, in many instances, features that are determinant for ligand-mediated protein interactions and, to further test its capabilities, we sought to *de novo* design this type of interactions.

bioRxiv preprint doi: https://doi.org/10.1101/2024.03.25.585721; this version posted March 28, 2024. The copyright holder for this preprint (which was not certified by peer review) is the author/funder, who has granted bioRxiv a license to display the preprint in perpetuity. It is made available under aCC-BY-NC-ND 4.0 International license.

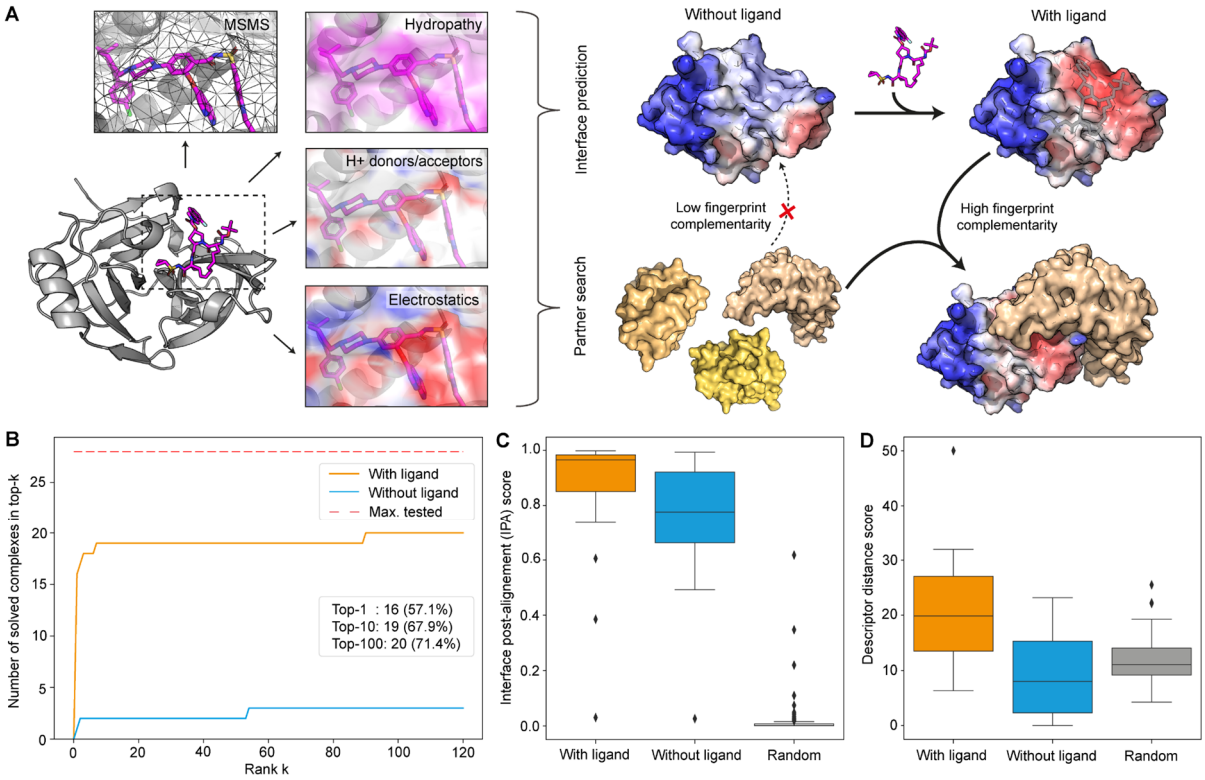

Fig. 1: Neosurface properties are captured to identify interface sites and binding partners. A. Geometric and chemical features of the ligand-protein complexes are computed, including the molecular surface representation (MSMS), hydropathy score, proton donors/acceptors and Poisson-Boltzmann electrostatics. Surface features are vectorized in a descriptor (also referred to as "fingerprint") and used by *MaSIF-neosurf* for interface propensity prediction or protein partner search. The ligand-containing fingerprint is then used to find complementary fingerprints in a patch database. **B.** Ranking predictions using *MaSIF-neosurf* on a benchmark dataset of known ternary complexes and a set of 200 decoys. Complementary partner search was performed in the presence (orange) and absence (blue) of the respective small molecule ligand. **C-D.** Interface post-alignment score (IPA; C) and descriptor distance score (see Methods; D) of the interacting complexes in the presence (orange) and absence (blue) of the drug compared to a set of random patch alignments (gray)

Designing novel ligand-induced protein interactions

Recently, we proposed the *MaSIF-seed* pipeline for the design of *de novo* site-specific protein binders(*28*). Given the performance of *MaSIF-seed* against multiple therapeutically relevant targets, we sought to test whether such an approach could generalize to design site-specific binders to neosurfaces composed of ligand and protein atoms. By doing so, we tackle the challenge of designing chemically controlled protein interactions and test our understanding of molecular recognition events mediated by neosurfaces. We therefore adapted our *MaSIF-seed* pipeline to our newly proposed *MaSIF-neosurf* framework (Fig. 2A). Once neosurfaces are computed for a given protein-ligand complex, we first take advantage of *MaSIF-site* to identify the regions most likely to become buried in an interface. Then an extensive fingerprint search identifies complementary structural motifs (i.e. binding seeds) from a database of

bioRxiv preprint doi: https://doi.org/10.1101/2024.03.25.585721; this version posted March 28, 2024. The copyright holder for this preprint (which was not certified by peer review) is the author/funder, who has granted bioRxiv a license to display the preprint in perpetuity. It is made available under aCC-BY-NC-ND 4.0 International license.

~640'000 structural fragments (402 million surface patches/fingerprints). Therefore, by focusing on the predicted buried regions of the interface and searching for highly complementary motifs, the vast space of patches and binding motifs is quickly reduced to the most promising candidates. Finally, the top seeds are refined by sequence optimization and grafted with Rosetta(*38*) on recipient proteins (i.e. scaffolds) to stabilize the binding motif. Lastly, a final round of sequence design is performed to improve atomic contacts at the interface.

We designed ligand-dependent protein binders targeting ligand-bound proteins from different families: Bcl2 in complex with the clinically approved drug Venetoclax; an anti-progesterone antibody (DB3) in complex with its ligand; and peptide deformylase 1 (PDF1) from *P. aeruginosa* in complex with the antibiotic Actinonin (Fig 2B). We first identified a moderate to high interface propensity of these neosurfaces with *MaSIF-neosurf*, selected 1 to 3 relevant interface patches depending on the solvent-accessible surface area exposed by the ligand (Fig. 2B), and searched for complementary fingerprints in our seed database. Top-ranking seeds were selected, refined, and grafted onto recipient scaffolds, and approximately 2000 designs per target complex were selected with computational filters (Fig. 2C and table S1, see Methods). Our pipeline generated designs with diverse helical and beta sheet-based binding motifs, as well as various protein folds, thus sampling a wide space of sequences and topologies (Fig. 2C). All selected designs were predicted to favorably engage the neosurface by showing increased interface structural metrics in the presence of the ligand, such as the predicted binding energy, the buried surface area and the number of atomic contacts (fig. S3).

Experimental validation of ligand-induced PPIs

The computational designs were screened by yeast display(*39*) and, after two rounds of fluorescent-activated cell sorting (FACS), enriched clones were deep sequenced (fig. S4 and table S2). We show one binder targeting each of the selected test cases (Fig. 3A). The best designs show no binding in the absence of the corresponding small molecules, whereas modest to high binding signals were observed with the ligands in yeast display experiments (Fig. 3B). These changes of binding signal upon small molecule addition are consistent with the expected behavior of a chemically induced PPI. Interestingly, small molecules contributed about 10-12% of the predicted target buried surface area, but they improved the predicted binding energy ($\Delta\Delta G$) of the interface compared to the ligand unbound form by 17% to 27.7%. This result demonstrates a small, yet critical contribution that each ligand plays in the binding event, highlighting the difficulty of the design problem (table S3).

bioRxiv preprint doi: https://doi.org/10.1101/2024.03.25.585721; this version posted March 28, 2024. The copyright holder for this preprint (which was not certified by peer review) is the author/funder, who has granted bioRxiv a license to display the preprint in perpetuity. It is made available under aCC-BY-NC-ND 4.0 International license.

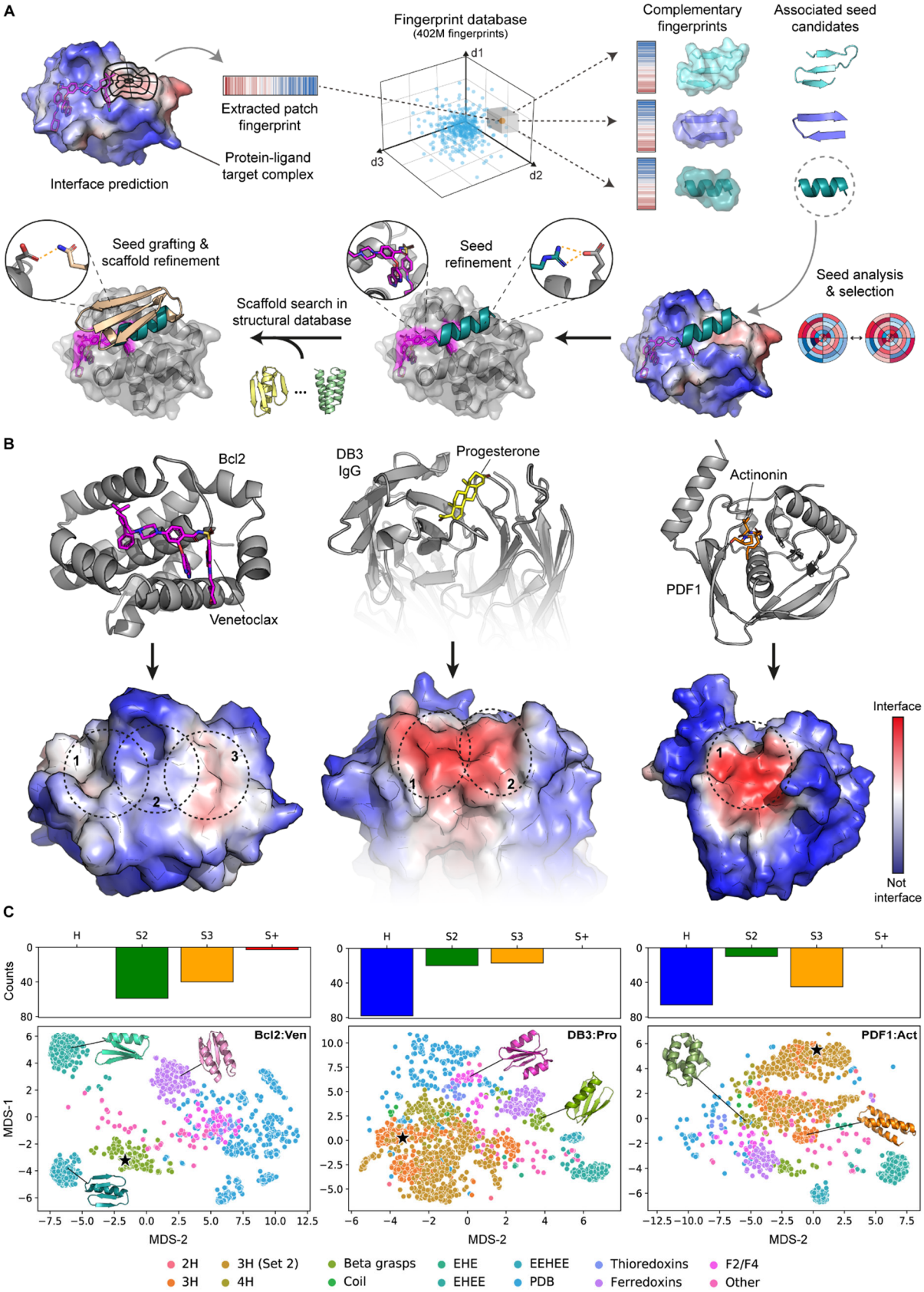

Fig. 2: Design of ligand-induced protein interactions with *MaSIF-neosurf*. A. To design novel ligand-induced protein interactions, potential interface sites are first identified on the target protein-ligand complex. The corresponding patches are then used to find complementary fingerprints in a patch database. The top patches are aligned and scored to refine the selection. Associated binding motifs (seeds) undergo sequence optimization with an emphasis on designing new hydrogen bond networks with the target protein and small molecule. Seeds are

bioRxiv preprint doi: https://doi.org/10.1101/2024.03.25.585721; this version posted March 28, 2024. The copyright holder for this preprint (which was not certified by peer review) is the author/funder, who has granted bioRxiv a license to display the preprint in perpetuity. It is made available under aCC-BY-NC-ND 4.0 International license.

then grafted on suitable scaffolds from a structural database, and the rest of the scaffold interface is redesigned using Rosetta. Finally, the top ~2000 designs, according to different structural metrics, are selected and screened experimentally. **B.** Target candidates in complex with their respective small molecules (top row). Neosurfaces displaying their protein binding propensity (bottom row). Sites selected for binder design are highlighted with dashed circles. **C.** Seed structural diversity (top row) includes motifs that are: helical (H); two-strand beta sheets (S2); three-strand beta sheets (S3); and more complex beta sheet motifs (S+). Diversity of the ~2000 computational designs (bottom row) mapped using multidimensional scaling (MDS) of pairwise RMSDs between all designs. Experimentally confirmed binders are highlighted with a star.

Moreover, point mutants at the interface hotspot residues abrogated binding to the target complex, which further supports the designed binding mode (Fig. 3C). No binding was observed with the native scaffolds used for the seed grafting and interface design, underlying the critical role of the interface design pipeline (Fig. 3C). Finally, specificity towards the desired ligand was confirmed by using control compounds: S55746 for Bcl2, 19-O-Benzoyl-Progesterone (OBz-Pro) for DB3 IgG and Tertbutyldimethylsilyl-Actinonin (TBDMS-Act) for PDF1 (Fig. 3D and fig. S5). These analogs retained binding to the protein target (fig. S5). However, no binding to the designs was observed, confirming that the correct interface on the target complex is engaged with high ligand specificity (Fig. 3D).

Biochemical characterization and structural validation

To map the binding site with high confidence and identify potential beneficial mutations (fig. S6), we performed a site-saturation mutagenesis (SSM) study (fig. S6). To assess the effect of the different mutations over the designed ligand-dependent interaction, we computed the average enrichment score of each mutation when comparing binding versus non-binding populations on yeast display experiments, similar to other deep saturation mutagenesis studies(*40*, *41*). Globally, we observed that such interactions have exquisite sensitivity to single-point mutants and that residues with high sensitivity mapped very closely to the designed interfaces, supporting the accuracy of our computational models (Fig. 4A).

The initial successful designs were expressed and purified for further biophysical characterization. All designs were monomeric, folded and highly stable in solution (fig. S7). All three designs showed binding affinities in the range of native transient PPIs(*42*), from mid-nanomolar to low-micromolar, after pure *in silico* generation (fig. S8). Specifically, DBAct553_1 showed a binding affinity (K_D) of 542 nM, DBVen1619_1 and DBPro1156_1 showed affinities of 4 μM and >10 μM, respectively.

bioRxiv preprint doi: https://doi.org/10.1101/2024.03.25.585721; this version posted March 28, 2024. The copyright holder for this preprint (which was not certified by peer review) is the author/funder, who has granted bioRxiv a license to display the preprint in perpetuity. It is made available under aCC-BY-NC-ND 4.0 International license.

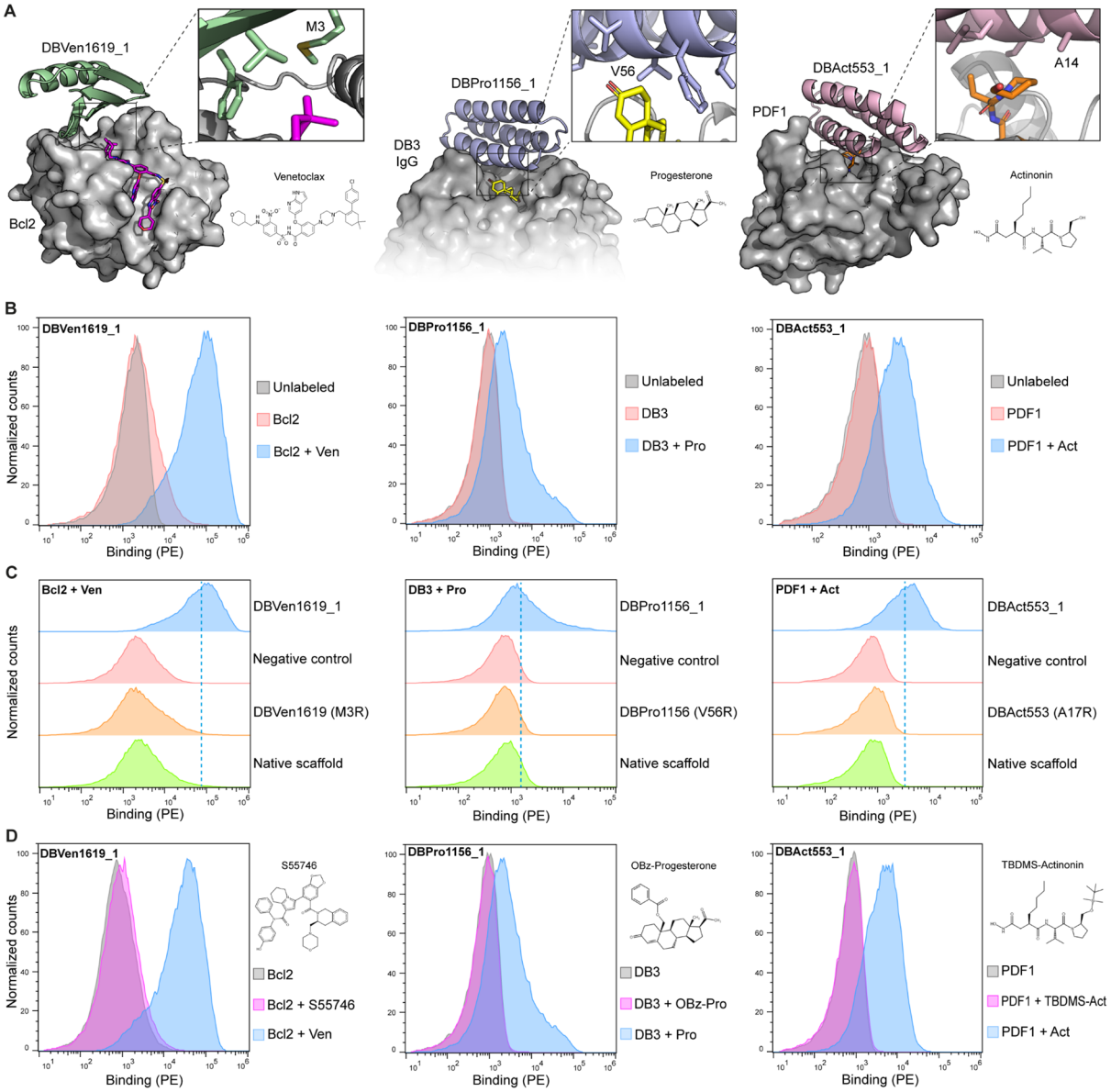

Fig. 3: *De novo* design and screening of small molecule-dependent binders. A. Models of the designed binders in complex with their respective target complexes: Bcl2:Venetoclax, DB3:Progesterone and PDF1:Actinonin **B.** Histograms of the binding signal (PE, phycoerythrin) measured by flow cytometry on yeast displaying the designed binders. Yeast were either unlabeled or labeled with 500 nM of their respective target protein preincubated with the ligand, or with the target protein alone. **C.** Histograms of the binding signal (PE, phycoerythrin) measured by flow cytometry on yeast displaying designed binders, a mutated version with a single point mutant at the predicted interface and the starting scaffold used for the design process. Yeast cells were labeled with 500 nM of their respective drug:protein complex. Dashed lines represent the geometric mean of the designed binder signal. **D.** Binding measured on yeast displaying DBVen1619_1, DBPro1156_1 or DBAct553_1 labeled with the target protein alone (gray), the target protein in complex with the original small molecule (blue), or the target protein in complex with the small molecule analog (magenta). Control analogs tested were S55746, Progesterone-19-O-Benzoyl (OBz-Pro) and Tertbutyldimethylsilyl-Actinonin (TBDMS-Act).

bioRxiv preprint doi: https://doi.org/10.1101/2024.03.25.585721; this version posted March 28, 2024. The copyright holder for this preprint (which was not certified by peer review) is the author/funder, who has granted bioRxiv a license to display the preprint in perpetuity. It is made available under aCC-BY-NC-ND 4.0 International license.

In the SSM scan, some mutations suggested potential improvements in affinity (fig. S6). Due to the large number of beneficial mutation candidates for DBVen1619_1, we created a combinatorial library covering 6 residues, sampling a set of favorable amino acids identified by SSM (fig. S9). Three of the six positions converged into single mutations (K1Q, M3L, I13K) while the remaining three residues did not converge. We engineered a variant, DBVen1619_2, with the three beneficial mutations and confirmed the binding improvement on yeast display (fig. S9). Among the favorable mutations, M3L in the core of the interface between Bcl2:Venetoclax and DBVen1619_2 plays a crucial role (Fig. 4B). The conformational rigidity of a leucine is likely to be preferred to the rotameric flexibility of a methionine(*43*), reducing the entropic cost of the binding interaction(*44*). On the other hand, the second beneficial mutation (I13K) is likely to provide a favorable electrostatic interaction with a glutamate nearby. Overall, the incorporation of the three mutations resulted in a 42-fold improvement of the affinity (K_D = 96 nM, Fig. 4C)

For the progesterone-dependent binder, DBPro1156_1, four favorable mutations were identified by SSM and showed an increased binding on yeast display (fig. S10). Two mutations (Y12W and S16G) significantly improved the binding signal and showed an additive effect in the resulting design, DBPro1156_2. Modeling of the two mutations suggested increased interface packing (Y12W) and the removal of a steric clash (S16G) (Fig. 4B, middle panel). DBPro1156_2 showed a binding affinity of 18 nM, which represents an improvement of three orders of magnitude, relative to the parent design, solely with two mutations (Fig. 4C).

Several mutations were found to slightly improve binding of DBAct553_1 to Actinonin-bound PDF1 (fig. S11). Most of these mutations were hypothesized to result in a more elaborate hydrogen bond network across the interface (e.g. R7N or A8R) (Fig. 4B). Of note, the combination of I3E with R7N was found to be deleterious for binding (fig. S11), most probably because of their spatial proximity that might trigger unwanted side chain rearrangement. A combination of the beneficial mutations (R7N and A8R) gave rise to DBAct553_2, which bound with an affinity of 446 nM for the Actinonin-bound PDF1 (Fig. 4C).

To evaluate the structural accuracy of our computational design approach, we co-crystalized the ternary complex of Actinonin-bound PDF1 with DBAct553_1 (PDB: 8S1X, Fig. 4D). The crystal structure closely resembled the computational model with a C_α RMSD (Root Mean Square Deviation) of 2.33 Å and a full-atom interface RMSD (iRMSD) of 2.26 Å, which demonstrates the accuracy of our design pipeline. The deviation from our initial model can to a large extent be attributed to a misplaced residue (Y2) in the model of the design scaffold which induced a slight shift of the N-terminal helix (fig. S12). Consequently, the C_α RMSD of

bioRxiv preprint doi: https://doi.org/10.1101/2024.03.25.585721; this version posted March 28, 2024. The copyright holder for this preprint (which was not certified by peer review) is the author/funder, who has granted bioRxiv a license to display the preprint in perpetuity. It is made available under aCC-BY-NC-ND 4.0 International license.

our model deviates 0.93 Å from that of the experimental structure (fig. S12). Of note, the AlphaFold2(*45*) prediction of the monomeric designed binder aligned perfectly with our structure with a C_α RMSD of 0.49 Å by placing residue Y2 with the correct orientation. Overall, this observation together with previous findings suggests that an increased use of deep learning tools like AlphaFold should significantly increase the model accuracy and therefore success rate(*46*). Finally, we obtained low-resolution cryo-electron microscopy densities of the DBPro1156_2 in complex with DB3 Fab and progesterone that confirmed the designed binding mode and interface engagement with the small molecule (Fig. 4E). Despite the absence of structural data for the remainder of the designs, the mutational sensitivity assessed by the SSM (Fig. 4A) and the lack of binding with the small molecule analogs (Fig. 3D) suggests that the binders engage the target interface with a binding mode in agreement with our computational models.

Designed CIDs are functional in cell-based systems

Chemically controllable components have important applications in synthetic biology and have been shown to be useful in modulating the activity of emerging cell-based therapies (*10*, *11*, *47*). To test whether our computationally designed CIDs would assemble in a more complex cellular context, we engineered reporter proximity-based systems that were expressed in cell-free system or mammalian cells and that in the presence of the small molecule could activate a signaling pathway or lead to the reconstitution of a reporter protein. The most natural functional logic for chemically-induced protein interactions is to function as ON-switch systems.

We first repurposed a previously described heterodimerization-based reporter system(*48*) to test the DB3 antibody as a single-chain variable fragment (scFv) binding to DBPro1156_2. Here, DB3 was fused to a zinc finger 438 transcription factor and DBAct553_2 to a T7 RNA polymerase (Fig. 5A), and tested in a cell-free reporter system. The heterodimerization in presence of the drug induces proximity between the T7 RNA polymerase and the transcription factor, thus leading to the transcription of a reporter linear DNA template and its translation into a red fluorescent protein (mCherry). While only baseline fluorescence was observed in absence of progesterone, a 15.8-fold increase was observed after addition of progesterone (Fig. 5B). Similarly, a titration of progesterone demonstrated a dose-response curve, suggesting possible utilization as a novel cell-free biosensor (Fig. 5C).

bioRxiv preprint doi: https://doi.org/10.1101/2024.03.25.585721; this version posted March 28, 2024. The copyright holder for this preprint (which was not certified by peer review) is the author/funder, who has granted bioRxiv a license to display the preprint in perpetuity. It is made available under aCC-BY-NC-ND 4.0 International license.

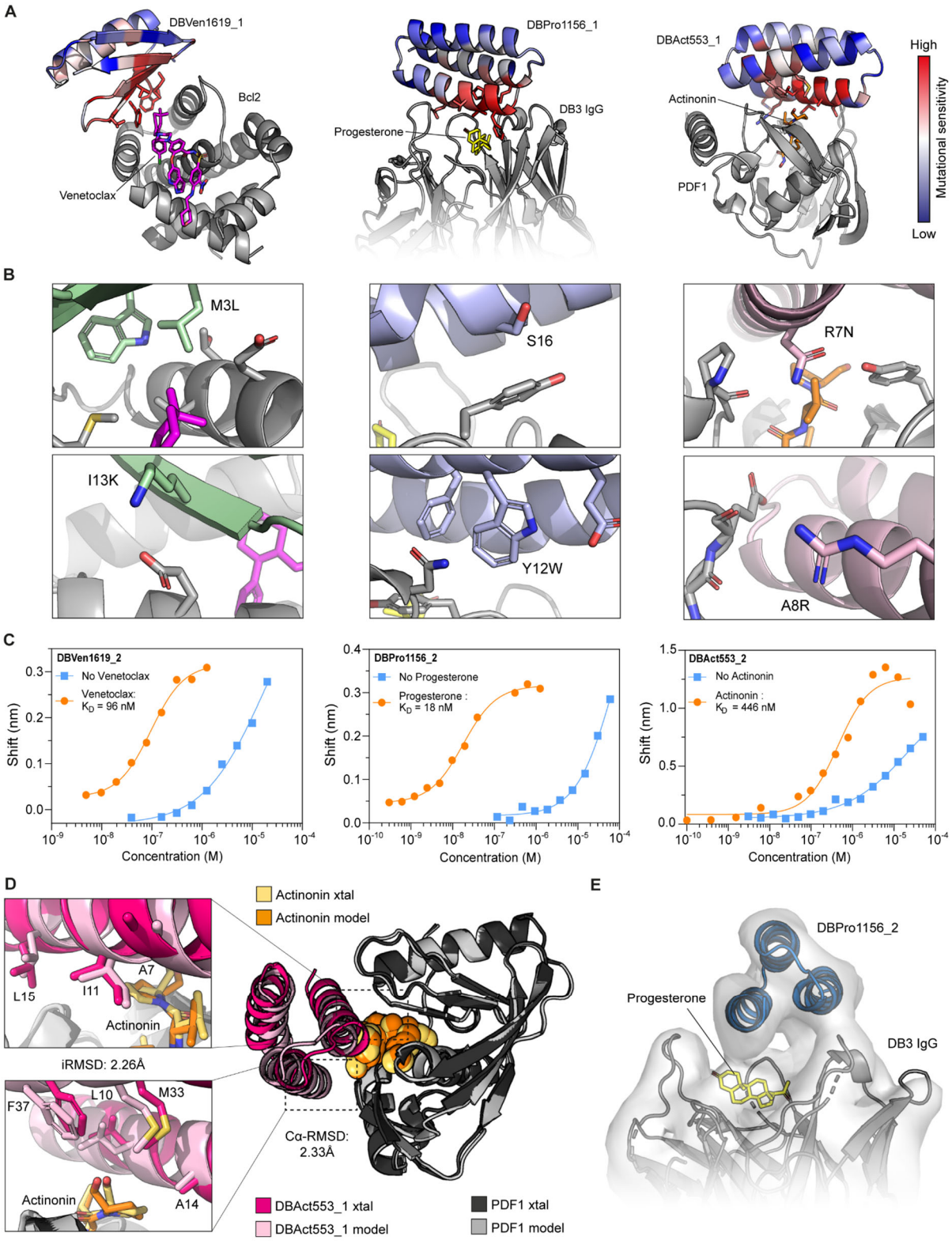

Fig. 4: Optimization, characterization and functionalization of the designed binders. A. Computational model colored with the average enrichment score of the site-saturation mutagenesis of each amino acid position of the designed binder. Red color suggests that an amino acid position is sensitive to mutations, while blue color highlights a more tolerant amino acid position. Target proteins are shown in gray. **B.** Computational models incorporating the beneficial mutations that improved the affinity of the designed binders. Target proteins are shown in gray and designed binders in their respective color. **C.** Affinity measurement for DBVen1619_2, DBPro1156_2 and DBAct553_2 performed by biolayer interferometry. Each measurement was performed in presence (orange) or absence (blue) of the respective small molecule. The fits were calculated using a nonlinear four-parameter curve

bioRxiv preprint doi: https://doi.org/10.1101/2024.03.25.585721; this version posted March 28, 2024. The copyright holder for this preprint (which was not certified by peer review) is the author/funder, who has granted bioRxiv a license to display the preprint in perpetuity. It is made available under aCC-BY-NC-ND 4.0 International license.

fitting analysis. **D.** Crystal (xtal) structure of DBAct553_1 in complex with Actinonin-bound PDF1 (PDB: 8S1X). The computational model (light pink) is aligned with the crystal structure (magenta). Inset: the alignment of the residues at the interface. E. Cryo-electron microscopy densities obtained for DBPro1156_2 in complex with progesterone-bound DB3.

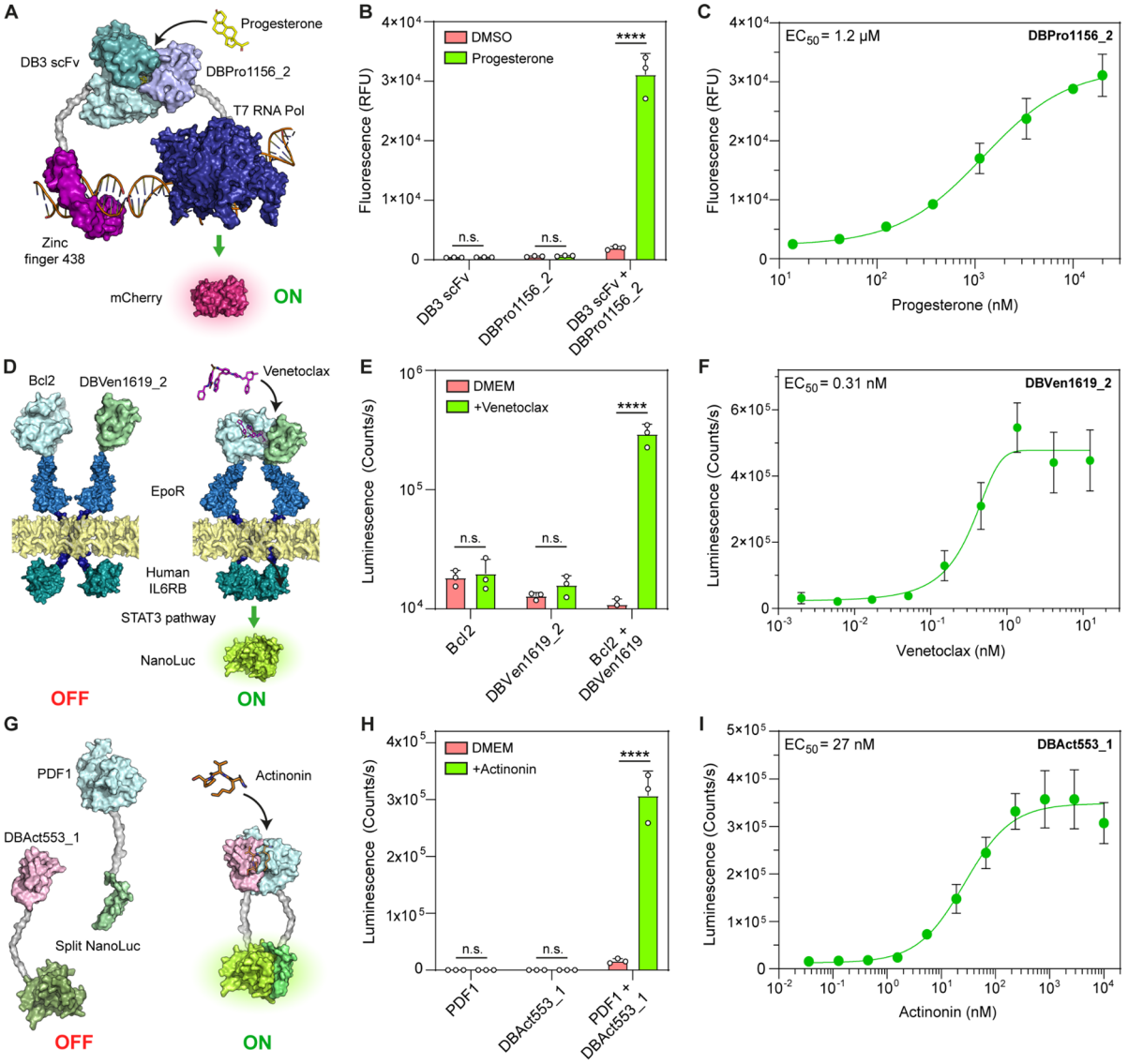

Fig. 5: Computationally designed CIDs are functional in cell-based systems. A. Schematic of the cell free-expression system with single chain variable fragment (scFv) DB3-fused to a zinc finger transcription factor and DBPro1156_2 fused to T7 RNA polymerase. **B.** Fluorescence (Relative fluorescence unit; RFU) measured in wells containing each monomeric component or mixed, without or with 20 µM progesterone. **C.** Progesterone dose-dependent responses performed in a cell free system containing both components. **D.** Schematic of the GEMS reporter system functionalizing Bcl2-based CID. Both protein components of the CID are individually fused to erythropoietin receptor (EpoR) chains linked to an intracellular human IL6RB domain, which induces the expression of a reporter gene (secreted NanoLuc luciferase) when activated. **E.** NanoLuc luminescence of HEK293 cells transfected with Bcl2-GEMS only, DBVen1619_2 only or both together without or with 1 µM Venetoclax. **F.** Venetoclax dose-dependent responses performed on HEK293 transfected with Bcl2 and DBV1619 GEMS receptors. **G.** Schematic of the split NanoLuc system functionalizing DBAct553_1 and PDF1. **H.** Intracellular NanoLuc luminescence of HEK293 transfected with C-term split NanoLuc-fused PDF1 only, N-term split NanoLuc-fused DBAct553_1 only or both together without or with 25µM Actinonin. **I.** Actinonin dose-dependent responses performed on HEK293 transfected with split-NanoLuc PDF1 and DBAct553_1. $p < 0.0001$ (****), non-significant (ns).

bioRxiv preprint doi: https://doi.org/10.1101/2024.03.25.585721; this version posted March 28, 2024. The copyright holder for this preprint (which was not certified by peer review) is the author/funder, who has granted bioRxiv a license to display the preprint in perpetuity. It is made available under aCC-BY-NC-ND 4.0 International license.

To test the chemically-induced activity of the designed modules in mammalian cells, we used a previously described system called generalized extracellular molecule sensor (GEMS)(*13*). Briefly, the target protein and the designed binder are both fused to an erythropoietin receptor (EpoR) linked to an intracellular domain of a human interleukin 6 receptor subunit B (IL6RB) (Fig. 5D). Transcription of a reporter gene (NanoLuc luciferase)(*49*) will be triggered upon a conformational change induced by the heterodimerization in presence of the drug. By incorporating Bcl2 and DBVen1619_2 in the GEMS system, we observed a 26.8-fold change in luminescence in the presence of Venetoclax, while minimal background was observed in the absence of the drug (Fig. 5E). These results show the desired behavior of an ON-switch system. Additionally, our modified GEMS system displayed a heightened sensitivity to the drug, with a half maximal effective concentration (EC_{50}) of 0.31 nM, which is likely due to the co-localization of the sensing modules in the cell membrane (Fig. 5F).

Next, we designed a cytoplasmic system to respond to Actinonin and fused PDF1 and DBAct553_1 to two moieties of a split NanoLuc (Fig. 5G). In this system we also observed a significant increase in signal (19.1-fold) upon dosing of the cells with Actinonin (Fig. 5H). This novel ON-switch system was also highly sensitive to the presence of the drug, as shown by the titration reporting an EC_{50} of 27 nM (Fig. 5I). Overall, we showed that our computationally designed CIDs can be used to functionalize molecular components in cellular systems, suggesting a promising route for the development of new modules for synthetic biology including a wide range of biosensors and cell-based applications.

Discussion

Current deep learning-based protein design pipelines are primarily conditioned on the natural amino acid repertoire(*50–52*) and therefore lack generalization to the design of interactions involving small molecules. This gap is mainly due to the scarcity of protein-ligand structural data, and especially ternary complexes, within the training sets based on the PDB, where such complexes are limited(*53–55*). Geometric deep learning approaches principled in the physical and chemical features of the molecular surface can overcome these limitations, and provide joint representations for protein and small molecule complexes. The resulting neosurfaces capture and present generalizable molecular features that enable the challenging task of designing protein binders targeting these hybrid interfaces. Utilizing the *MaSIF-neosurf* framework, we successfully designed three specific binders against Bcl2:Venetoclax, DB3:Progesterone and PDF1:Actinonin complexes. All designed binders showed high stability, specificity and native-like affinity for their target complexes by pure *in silico* generation. The affinities were experimentally optimized to nanomolar range and their binding

bioRxiv preprint doi: https://doi.org/10.1101/2024.03.25.585721; this version posted March 28, 2024. The copyright holder for this preprint (which was not certified by peer review) is the author/funder, who has granted bioRxiv a license to display the preprint in perpetuity. It is made available under aCC-BY-NC-ND 4.0 International license.

mode was confirmed through mutational and structural characterization, showcasing the accuracy of our design pipeline. Notably, our pipeline managed to capture the subtle, yet crucial contributions of each ligand (10-12% of the buried SASA only; table S3) to induce protein interactions. This sensitivity represents an additional layer of complexity to the task of designing highly sensitive CIDs, compared to previous attempts targeting large ligand interfaces(*26*).

To demonstrate the functionality of our designed CID systems, we probed their efficiency and specificity in the context of a complex cellular environment. They exhibited robust ON-switch behavior in both cytoplasmic and membrane-bound circuits, showcasing their potentially wide applicability in mammalian systems as logic gates, synthetic circuits, or new biosensors for detecting specific metabolites(*10*, *13*). This relevance is further underscored by our use of the FDA-approved drug Venetoclax for treating leukemia(*29*) the natural product Actinonin with potentially chemotherapeutic effects (*31*) or the endogenous hormone progesterone (*56*). These can be utilized for combined anti-cancer therapies with chimeric antigen receptor (CAR) T cells, which are often hindered by off-target toxicities (*11*, *57*). The addition of synthetic small molecule activators could allow finer control of their activity and elevate their safety profile.

While the design of specific protein-ligand interactions remains challenging, the presented results lay a strong foundation for further innovations. Incorporation of deep learning-based structure validation methods, such as AlphaFold2(*45*) (fig. S13) or RoseTTAFold(*58*), or generative models complemented with surface fingerprints(*51*) could improve design success rates. Additionally, accounting for conformational flexibility and dynamics at the surface could pave the way for more complex interaction types, such as intrinsically disordered proteins. Overall, we envision that surface-based representation can contribute to solving molecular design problems in low-data regimens, such as the design of protein-based molecules with non-natural amino acids. The capability of extracting expressive fingerprints from protein:ligand complexes opens up the tantalizing possibility of rationally designing innovative drug modalities, such as on-command cell-based therapies(*11*, *17*), controllable biologics(*21*, *23*), or molecular glues, which thus far remains an outstanding challenge in drug development(*8*, *9*)

bioRxiv preprint doi: https://doi.org/10.1101/2024.03.25.585721; this version posted March 28, 2024. The copyright holder for this preprint (which was not certified by peer review) is the author/funder, who has granted bioRxiv a license to display the preprint in perpetuity. It is made available under aCC-BY-NC-ND 4.0 International license.

References

1. J. Janin, R. P. Bahadur, P. Chakrabarti, Protein–protein interaction and quaternary structure. *Q. Rev. Biophys.* **41**, 133–180 (2008).
2. M. W. Gonzalez, M. G. Kann, Chapter 4: Protein Interactions and Disease. *PLOS Comput. Biol.* **8**, e1002819 (2012).
3. A. Marchand, A. K. Van Hall-Beauvais, B. E. Correia, Computational design of novel protein–protein interactions – An overview on methodological approaches and applications. *Curr. Opin. Struct. Biol.* **74**, 102370 (2022).
4. J. Monod, J.-P. Changeux, F. Jacob, Allosteric proteins and cellular control systems. *J. Mol. Biol.* **6**, 306–329 (1963).
5. B. T. Seet, I. Dikic, M.-M. Zhou, T. Pawson, Reading protein modifications with interaction domains. *Nat. Rev. Mol. Cell Biol.* **7**, 473–483 (2006).
6. D. Patel, J. Kopec, F. Fitzpatrick, T. J. McCorvie, W. W. Yue, Structural basis for ligand-dependent dimerization of phenylalanine hydroxylase regulatory domain. *Sci. Rep.* **6**, 23748 (2016).
7. J. Schlessinger, Ligand-Induced, Receptor-Mediated Dimerization and Activation of EGF Receptor. *Cell* **110**, 669–672 (2002).
8. S. L. Schreiber, The Rise of Molecular Glues. *Cell* **184**, 3–9 (2021).
9. V. Oleinikovas, P. Gainza, T. Ryckmans, B. Fasching, N. H. Thomä, From Thalidomide to Rational Molecular Glue Design for Targeted Protein Degradation. *Annu. Rev. Pharmacol. Toxicol.* **64**, 291–312 (2024).
10. S. Shui, S. Buckley, L. Scheller, B. E. Correia, Rational design of small-molecule responsive protein switches. *Protein Sci.* **32**, e4774 (2023).
11. G. Giordano-Attianese, P. Gainza, E. Gray-Gaillard, E. Cribioli, S. Shui, S. Kim, M.-J. Kwak, S. Vollers, A. D. J. Corria Osorio, P. Reichenbach, J. Bonet, B.-H. Oh, M. Irving, G. Coukos, B. E. Correia, A computationally designed chimeric antigen receptor provides a small-molecule safety switch for T-cell therapy. *Nat. Biotechnol.* **38**, 426–432 (2020).
12. S. Shui, P. Gainza, L. Scheller, C. Yang, Y. Kurumida, S. Rosset, S. Georgeon, R. B. Di Roberto, R. Castellanos-Rueda, S. T. Reddy, B. E. Correia, A rational blueprint for the design of chemically-controlled protein switches. *Nat. Commun.* **12**, 5754 (2021).
13. L. Scheller, T. Strittmatter, D. Fuchs, D. Bojar, M. Fussenegger, Generalized extracellular molecule sensor platform for programming cellular behavior. *Nat. Chem. Biol.* **14**, 723–729 (2018).
14. N. D. Taylor, A. S. Garruss, R. Moretti, S. Chan, M. A. Arbing, D. Cascio, J. K. Rogers, F. J. Isaacs, S. Kosuri, D. Baker, S. Fields, G. M. Church, S. Raman, Engineering an allosteric transcription factor to respond to new ligands. *Nat. Methods* **13**, 177–183 (2016).
15. M. Békés, D. R. Langley, C. M. Crews, PROTAC targeted protein degraders: the past is prologue. *Nat. Rev. Drug Discov.* **21**, 181–200 (2022).
16. J. A. Wells, K. Kumru, Extracellular targeted protein degradation: an emerging modality for drug discovery. *Nat. Rev. Drug Discov.*, doi: 10.1038/s41573-023-00833-z (2023).
17. M. Jan, I. Scarfò, R. C. Larson, A. Walker, A. Schmidts, A. A. Guirguis, J. A. Gasser, M. Słabicki, A. A. Bouffard, A. P. Castano, M. C. Kann, M. L. Cabral, A. Tepper, D. E. Grinshpun, A. S. Sperling, T. Kyung, Q. L. Sievers, M. E. Birnbaum, M. V. Maus, B. L. Ebert, Reversible ON- and OFF-switch chimeric antigen receptors controlled by lenalidomide. *Sci. Transl. Med.* **13**, eabb6295 (2021).
18. M. Ishida, H. Watanabe, K. Takigawa, Y. Kurishita, C. Oki, A. Nakamura, I. Hamachi, S. Tsukiji, Synthetic Self-Localizing Ligands That Control the Spatial Location of Proteins in Living Cells. *J. Am. Chem. Soc.* **135**, 12684–12689 (2013).
19. W. J. Gibson, A. Sadagopan, V. M. Shoba, A. Choudhary, M. Meyerson, S. L. Schreiber, Bifunctional Small Molecules That Induce Nuclear Localization and Targeted Transcriptional Regulation. *J. Am. Chem. Soc.* **145**, 26028–26037 (2023).
20. C. S. C. Ng, A. Liu, B. Cui, S. M. Banik, “Targeted Protein Relocalization via Protein

bioRxiv preprint doi: https://doi.org/10.1101/2024.03.25.585721; this version posted March 28, 2024. The copyright holder for this preprint (which was not certified by peer review) is the author/funder, who has granted bioRxiv a license to display the preprint in perpetuity. It is made available under aCC-BY-NC-ND 4.0 International license.

Transport Coupling" (preprint, Biochemistry, 2023); https://doi.org/10.1101/2023.10.04.560943.

21. A. Marchand, L. Bonati, S. Shui, L. Scheller, P. Gainza, S. Rosset, S. Georgeon, L. Tang, B. E. Correia, Rational Design of Chemically Controlled Antibodies and Protein Therapeutics. *ACS Chem. Biol.* **18**, 1259–1265 (2023).
22. M. Mata, C. Gerken, P. Nguyen, G. Krenciute, D. M. Spencer, S. Gottschalk, Inducible Activation of MyD88 and CD40 in CAR T Cells Results in Controllable and Potent Antitumor Activity in Preclinical Solid Tumor Models. *Cancer Discov.* **7**, 1306–1319 (2017).
23. A. J. Martinko, E. F. Simonds, S. Prasad, A. Ponce, C. J. Bracken, J. Wei, Y.-H. Wang, T.-L. Chow, Z. Huang, M. J. Evans, J. A. Wells, Z. B. Hill, Switchable assembly and function of antibody complexes in vivo using a small molecule. *Proc. Natl. Acad. Sci.* **119**, e2117402119 (2022).
24. D. M. Spencer, T. J. Wandless, S. L. Schreiber, G. R. Crabtree, Controlling Signal Transduction with Synthetic Ligands. *Science* **262**, 1019–1024 (1993).
25. A. A. Glasgow, Y.-M. Huang, D. J. Mandell, M. Thompson, R. Ritterson, A. L. Loshbaugh, J. Pellegrino, C. Krivacic, R. A. Pache, K. A. Barlow, N. Ollikainen, D. Jeon, M. J. S. Kelly, J. S. Fraser, T. Kortemme, Computational design of a modular protein sense-response system. *Science* **366**, 1024–1028 (2019).
26. G. W. Foight, Z. Wang, C. T. Wei, P. Jr Greisen, K. M. Warner, D. Cunningham-Bryant, K. Park, T. J. Brunette, W. Sheffler, D. Baker, D. J. Maly, Multi-input chemical control of protein dimerization for programming graded cellular responses. *Nat. Biotechnol.* **37**, 1209–1216 (2019).
27. P. Gainza, F. Sverrisson, F. Monti, E. Rodolà, D. Boscaini, M. M. Bronstein, B. E. Correia, Deciphering interaction fingerprints from protein molecular surfaces using geometric deep learning. *Nat. Methods* **17**, 184–192 (2020).
28. P. Gainza, S. Wehrle, A. Van Hall-Beauvais, A. Marchand, A. Scheck, Z. Harteveld, S. Buckley, D. Ni, S. Tan, F. Sverrisson, C. Goverde, P. Turelli, C. Raclot, A. Teslenko, M. Pacesa, S. Rosset, S. Georgeon, J. Marsden, A. Petruzzella, K. Liu, Z. Xu, Y. Chai, P. Han, G. F. Gao, E. Oricchio, B. Fierz, D. Trono, H. Stahlberg, M. Bronstein, B. E. Correia, De novo design of protein interactions with learned surface fingerprints. *Nature* **617**, 176–184 (2023).
29. A. W. Roberts, M. S. Davids, J. M. Pagel, B. S. Kahl, S. D. Puvvada, J. F. Gerecitano, T. J. Kipps, M. A. Anderson, J. R. Brown, L. Gressick, S. Wong, M. Dunbar, M. Zhu, M. B. Desai, E. Cerri, S. Heitner Enschede, R. A. Humerickhouse, W. G. Wierda, J. F. Seymour, Targeting BCL2 with Venetoclax in Relapsed Chronic Lymphocytic Leukemia. *N. Engl. J. Med.* **374**, 311–322 (2016).
30. J. H. Arevalo, E. A. Stura, M. J. Taussig, I. A. Wilson, Three-dimensional Structure of an Anti-steroid Fab′ and Progesterone-Fab′ Complex. *J. Mol. Biol.* **231**, 103–118 (1993).
31. D. Z. Chen, D. V. Patel, C. J. Hackbarth, W. Wang, G. Dreyer, D. C. Young, P. S. Margolis, C. Wu, Z.-J. Ni, J. Trias, R. J. White, Z. Yuan, Actinonin, a Naturally Occurring Antibacterial Agent, Is a Potent Deformylase Inhibitor. *Biochemistry* **39**, 1256–1262 (2000).
32. J. J. Koenderink, A. J. van Doorn, Surface shape and curvature scales. *Image Vis. Comput.* **10**, 557–564 (1992).
33. Yin Shuangye, Proctor Elizabeth A., Lugovskoy Alexey A., Dokholyan Nikolay V., Fast screening of protein surfaces using geometric invariant fingerprints. *Proc. Natl. Acad. Sci.* **106**, 16622–16626 (2009).
34. A. V. Morozov, T. Kortemme, "Potential Functions for Hydrogen Bonds in Protein Structure Prediction and Design" in *Advances in Protein Chemistry* (Academic Press, 2005; https://www.sciencedirect.com/science/article/pii/S0065323305720015)vol. 72, pp. 1–38.
35. J. Kyte, R. F. Doolittle, A simple method for displaying the hydropathic character of a protein. *J. Mol. Biol.* **157**, 105–132 (1982).

bioRxiv preprint doi: https://doi.org/10.1101/2024.03.25.585721; this version posted March 28, 2024. The copyright holder for this preprint (which was not certified by peer review) is the author/funder, who has granted bioRxiv a license to display the preprint in perpetuity. It is made available under aCC-BY-NC-ND 4.0 International license.

36. S. A. Wildman, G. M. Crippen, Prediction of Physicochemical Parameters by Atomic Contributions. *J. Chem. Inf. Comput. Sci.* **39**, 868–873 (1999).
37. D. Eisenberg, E. Schwarz, M. Komaromy, R. Wall, Analysis of membrane and surface protein sequences with the hydrophobic moment plot. *J. Mol. Biol.* **179**, 125–142 (1984).
38. S. J. Fleishman, A. Leaver-Fay, J. E. Corn, E.-M. Strauch, S. D. Khare, N. Koga, J. Ashworth, P. Murphy, F. Richter, G. Lemmon, J. Meiler, D. Baker, RosettaScripts: A Scripting Language Interface to the Rosetta Macromolecular Modeling Suite. *PLOS ONE* **6**, e20161 (2011).
39. G. Chao, W. L. Lau, B. J. Hackel, S. L. Sazinsky, S. M. Lippow, K. D. Wittrup, Isolating and engineering human antibodies using yeast surface display. *Nat. Protoc.* **1**, 755–768 (2006).
40. L. Cao, I. Goreshnik, B. Coventry, J. B. Case, L. Miller, L. Kozodoy, R. E. Chen, L. Carter, A. C. Walls, Y.-J. Park, E.-M. Strauch, L. Stewart, M. S. Diamond, D. Veesler, D. Baker, De novo design of picomolar SARS-CoV-2 miniprotein inhibitors. *Science* **370**, 426–431 (2020).
41. L. Cao, B. Coventry, I. Goreshnik, B. Huang, W. Sheffler, J. S. Park, K. M. Jude, I. Marković, R. U. Kadam, K. H. G. Verschueren, K. Verstraete, S. T. R. Walsh, N. Bennett, A. Phal, A. Yang, L. Kozodoy, M. DeWitt, L. Picton, L. Miller, E.-M. Strauch, N. D. DeBouver, A. Pires, A. K. Bera, S. Halabiya, B. Hammerson, W. Yang, S. Bernard, L. Stewart, I. A. Wilson, H. Ruohola-Baker, J. Schlessinger, S. Lee, S. N. Savvides, K. C. Garcia, D. Baker, Design of protein-binding proteins from the target structure alone. *Nature* **605**, 551–560 (2022).
42. J. R. Perkins, I. Diboun, B. H. Dessailly, J. G. Lees, C. Orengo, Transient Protein-Protein Interactions: Structural, Functional, and Network Properties. *Structure* **18**, 1233–1243 (2010).
43. R. Najmanovich, J. Kuttner, V. Sobolev, M. Edelman, Side-chain flexibility in proteins upon ligand binding. *Proteins Struct. Funct. Genet.* **39**, 261–268 (2000).
44. C. Bissantz, B. Kuhn, M. Stahl, A Medicinal Chemist's Guide to Molecular Interactions. *J. Med. Chem.* **53**, 5061–5084 (2010).
45. J. Jumper, R. Evans, A. Pritzel, T. Green, M. Figurnov, O. Ronneberger, K. Tunyasuvunakool, R. Bates, A. Žídek, A. Potapenko, A. Bridgland, C. Meyer, S. A. A. Kohl, A. J. Ballard, A. Cowie, B. Romera-Paredes, S. Nikolov, R. Jain, J. Adler, T. Back, S. Petersen, D. Reiman, E. Clancy, M. Zielinski, M. Steinegger, M. Pacholska, T. Berghammer, S. Bodenstein, D. Silver, O. Vinyals, A. W. Senior, K. Kavukcuoglu, P. Kohli, D. Hassabis, Highly accurate protein structure prediction with AlphaFold. *Nature* **596**, 583–589 (2021).
46. N. R. Bennett, B. Coventry, I. Goreshnik, B. Huang, A. Allen, D. Vafeados, Y. P. Peng, J. Dauparas, M. Baek, L. Stewart, F. DiMaio, S. De Munck, S. N. Savvides, D. Baker, Improving de novo protein binder design with deep learning. *Nat. Commun.* **14**, 2625 (2023).
47. S. Shui, L. Scheller, B. E. Correia, Protein-based bandpass filters for controlling cellular signaling with chemical inputs. *Nat. Chem. Biol.*, doi: 10.1038/s41589-023-01463-7 (2023).
48. B. J. Hussey, D. R. McMillen, Programmable T7-based synthetic transcription factors. *Nucleic Acids Res.* **46**, 9842–9854 (2018).
49. C. G. England, E. B. Ehlerding, W. Cai, NanoLuc: A Small Luciferase Is Brightening Up the Field of Bioluminescence. *Bioconjug. Chem.* **27**, 1175–1187 (2016).
50. H. Khakzad, I. Igashov, A. Schneuing, C. Goverde, M. Bronstein, B. Correia, A new age in protein design empowered by deep learning. *Cell Syst.* **14**, 925–939 (2023).
51. J. L. Watson, D. Juergens, N. R. Bennett, B. L. Trippe, J. Yim, H. E. Eisenach, W. Ahern, A. J. Borst, R. J. Ragotte, L. F. Milles, B. I. M. Wicky, N. Hanikel, S. J. Pellock, A. Courbet, W. Sheffler, J. Wang, P. Venkatesh, I. Sappington, S. V. Torres, A. Lauko, V. De Bortoli, E. Mathieu, S. Ovchinnikov, R. Barzilay, T. S. Jaakkola, F. DiMaio, M. Baek, D. Baker, De novo design of protein structure and function with RFdiffusion.

bioRxiv preprint doi: https://doi.org/10.1101/2024.03.25.585721; this version posted March 28, 2024. The copyright holder for this preprint (which was not certified by peer review) is the author/funder, who has granted bioRxiv a license to display the preprint in perpetuity. It is made available under aCC-BY-NC-ND 4.0 International license.

Nature **620**, 1089–1100 (2023).
52. J. Dauparas, I. Anishchenko, N. Bennett, H. Bai, R. J. Ragotte, L. F. Milles, B. I. M. Wicky, A. Courbet, R. J. De Haas, N. Bethel, P. J. Y. Leung, T. F. Huddy, S. Pellock, D. Tischer, F. Chan, B. Koepnick, H. Nguyen, A. Kang, B. Sankaran, A. K. Bera, N. P. King, D. Baker, Robust deep learning–based protein sequence design using ProteinMPNN. *Science* **378**, 49–56 (2022).
53. H. Rui, K. S. Ashton, J. Min, C. Wang, P. R. Potts, Protein–protein interfaces in molecular glue-induced ternary complexes: classification, characterization, and prediction. *RSC Chem. Biol.* **4**, 192–215 (2023).
54. R. Ferreira De Freitas, M. Schapira, A systematic analysis of atomic protein–ligand interactions in the PDB. *MedChemComm* **8**, 1970–1981 (2017).
55. O. Orasch, N. Weber, M. Müller, A. Amanzadi, C. Gasbarri, C. Trummer, Protein–Protein Interaction Prediction for Targeted Protein Degradation. *Int. J. Mol. Sci.* **23**, 7033 (2022).
56. B. Nagy, J. Szekeres-Barthó, G. L. Kovács, E. Sulyok, B. Farkas, Á. Várnagy, V. Vértes, K. Kovács, J. Bódis, Key to Life: Physiological Role and Clinical Implications of Progesterone. *Int. J. Mol. Sci.* **22**, 11039 (2021).
57. R. A. Morgan, J. C. Yang, M. Kitano, M. E. Dudley, C. M. Laurencot, S. A. Rosenberg, Case Report of a Serious Adverse Event Following the Administration of T Cells Transduced With a Chimeric Antigen Receptor Recognizing ERBB2. *Mol. Ther.* **18**, 843–851 (2010).
58. R. Krishna, J. Wang, W. Ahern, P. Sturmfels, P. Venkatesh, I. Kalvet, G. R. Lee, F. S. Morey-Burrows, I. Anishchenko, I. R. Humphreys, R. McHugh, D. Vafeados, X. Li, G. A. Sutherland, A. Hitchcock, C. N. Hunter, A. Kang, E. Brackenbrough, A. K. Bera, M. Baek, F. DiMaio, D. Baker, Generalized biomolecular modeling and design with RoseTTAFold All-Atom. *Science*, eadl2528 (2024).
59. M. F. Sanner, A. J. Olson, J. C. Spehner, Reduced surface: an efficient way to compute molecular surfaces. *Biopolymers* **38**, 305–320 (1996).
60. E. Jurrus, D. Engel, K. Star, K. Monson, J. Brandi, L. E. Felberg, D. H. Brookes, L. Wilson, J. Chen, K. Liles, M. Chun, P. Li, D. W. Gohara, T. Dolinsky, R. Konecny, D. R. Koes, J. E. Nielsen, T. Head-Gordon, W. Geng, R. Krasny, G. Wei, M. J. Holst, J. A. McCammon, N. A. Baker, Improvements to the APBS biomolecular solvation software suite. *Protein Sci.* **27**, 112–128 (2018).
61. G. Landrum, RDKit.org, *RDKit: Open-source cheminformatics.* https://www.rdkit.org/.
62. J. Degen, C. Wegscheid-Gerlach, A. Zaliani, M. Rarey, On the Art of Compiling and Using "Drug-Like" Chemical Fragment Spaces. *ChemMedChem* **3**, 1503–1507 (2008).
63. L. Hu, M. L. Benson, R. D. Smith, M. G. Lerner, H. A. Carlson, Binding MOAD (Mother Of All Databases). *Proteins Struct. Funct. Bioinforma.* **60**, 333–340 (2005).
64. B. Coventry, D. Baker, Protein sequence optimization with a pairwise decomposable penalty for buried unsatisfied hydrogen bonds. *PLOS Comput. Biol.* **17**, e1008061 (2021).
65. D.-A. Silva, B. E. Correia, E. Procko, "Motif-Driven Design of Protein–Protein Interfaces" in *Computational Design of Ligand Binding Proteins*, B. L. Stoddard, Ed. (Springer New York, New York, NY, 2016; http://link.springer.com/10.1007/978-1-4939-3569-7_17)vol. 1414 of *Methods in Molecular Biology*, pp. 285–304.
66. H. M. Berman, The Protein Data Bank. *Nucleic Acids Res.* **28**, 235–242 (2000).
67. Rocklin Gabriel J., Chidyausiku Tamuka M., Goreshnik Inna, Ford Alex, Houliston Scott, Lemak Alexander, Carter Lauren, Ravichandran Rashmi, Mulligan Vikram K., Chevalier Aaron, Arrowsmith Cheryl H., Baker David, Global analysis of protein folding using massively parallel design, synthesis, and testing. *Science* **357**, 168–175 (2017).
68. G. Bhardwaj, V. K. Mulligan, C. D. Bahl, J. M. Gilmore, P. J. Harvey, O. Cheneval, G. W. Buchko, S. V. S. R. K. Pulavarti, Q. Kaas, A. Eletsky, P.-S. Huang, W. A. Johnsen, P. J. Greisen, G. J. Rocklin, Y. Song, T. W. Linsky, A. Watkins, S. A. Rettie, X. Xu, L. P. Carter, R. Bonneau, J. M. Olson, E. Coutsias, C. E. Correnti, T. Szyperski, D. J. Craik, D. Baker, Accurate de novo design of hyperstable constrained peptides. *Nature* **538**,

bioRxiv preprint doi: https://doi.org/10.1101/2024.03.25.585721; this version posted March 28, 2024. The copyright holder for this preprint (which was not certified by peer review) is the author/funder, who has granted bioRxiv a license to display the preprint in perpetuity. It is made available under aCC-BY-NC-ND 4.0 International license.

329–335 (2016).
69. A. R. Tobin, R. Crow, D. V. Urusova, J. C. Klima, N. H. Tolia, E. Strauch, Inhibition of a malaria host–pathogen interaction by a computationally designed inhibitor. *Protein Sci.* **32**, e4507 (2023).
70. T. W. Linsky, K. Noble, A. R. Tobin, R. Crow, L. Carter, J. L. Urbauer, D. Baker, E.-M. Strauch, Sampling of structure and sequence space of small protein folds. *Nat. Commun.* **13**, 7151 (2022).
71. Ö. Kartal, F. Andres, M. P. Lai, R. Nehme, K. Cottier, waveRAPID—A Robust Assay for High-Throughput Kinetic Screens with the Creoptix WAVEsystem. *SLAS Discov.* **26**, 995–1003 (2021).
72. L. Scheller, “Synthetic Receptors for Sensing Soluble Molecules with Mammalian Cells” in *Mammalian Cell Engineering*, R. Kojima, Ed. (Springer US, New York, NY, 2021; https://link.springer.com/10.1007/978-1-0716-1441-9_2)vol. 2312 of *Methods in Molecular Biology*, pp. 15–33.
73. W. Kabsch, *XDS*. *Acta Crystallogr. D Biol. Crystallogr.* **66**, 125–132 (2010).
74. Z. Otwinowski, W. Minor, Processing of X-ray diffraction data collected in oscillation mode. *Methods Enzym.* **276**, 307–326 (1997).
75. P. Emsley, K. Cowtan, Coot: model-building tools for molecular graphics. *Acta Crystallogr. D Biol. Crystallogr.* **60**, 2126–2132 (2004).
76. P. D. Adams, P. V. Afonine, G. Bunkóczi, V. B. Chen, I. W. Davis, N. Echols, J. J. Headd, L.-W. Hung, G. J. Kapral, R. W. Grosse-Kunstleve, A. J. McCoy, N. W. Moriarty, R. Oeffner, R. J. Read, D. C. Richardson, J. S. Richardson, T. C. Terwilliger, P. H. Zwart, PHENIX: a comprehensive Python-based system for macromolecular structure solution. *Acta Crystallogr. D Biol. Crystallogr.* **66**, 213–221 (2010).
77. V. B. Chen, W. B. Arendall, J. J. Headd, D. A. Keedy, R. M. Immormino, G. J. Kapral, L. W. Murray, J. S. Richardson, D. C. Richardson, MolProbity: all-atom structure validation for macromolecular crystallography. *Acta Crystallogr. D Biol. Crystallogr.* **66**, 12–21 (2010).
78. L. E. Macdonald, K. A. Meagher, M. C. Franklin, N. Levenkova, J. Hansen, A. T. Badithe, M. Zhong, P. Krueger, A. Rafique, N. Tu, J. Shevchuk, S. Wadhwa, G. Ehrlich, J. Bautista, C. Grant, L. Esau, W. T. Poueymirou, W. Auerbach, L. Morton, R. Babb, G. Chen, T. Huang, D. MacDonald, K. Graham, C. Gurer, V. A. Voronina, J. R. McWhirter, C. Guo, G. D. Yancopoulos, A. J. Murphy, Kappa-on-Heavy (KoH) bodies are a distinct class of fully-human antibody-like therapeutic agents with antigen-binding properties. *Proc. Natl. Acad. Sci.* **117**, 292–299 (2020).
79. T. D. Goddard, C. C. Huang, E. C. Meng, E. F. Pettersen, G. S. Couch, J. H. Morris, T. E. Ferrin, UCSF ChimeraX: Meeting modern challenges in visualization and analysis. *Protein Sci.* **27**, 14–25 (2018).
80. A. T. McNutt, P. Francoeur, R. Aggarwal, T. Masuda, R. Meli, M. Ragoza, J. Sunseri, D. R. Koes, GNINA 1.0: molecular docking with deep learning. *J. Cheminformatics* **13**, 43 (2021).

bioRxiv preprint doi: https://doi.org/10.1101/2024.03.25.585721; this version posted March 28, 2024. The copyright holder for this preprint (which was not certified by peer review) is the author/funder, who has granted bioRxiv a license to display the preprint in perpetuity. It is made available under aCC-BY-NC-ND 4.0 International license.

Acknowledgments

We would like to thank the staff at PTPSP at EPFL, Florence Pojer, Kelvin Lau, Amédé Larabi, Laurence Durrer and Soraya Quinche for their advice on the biophysical characterization of proteins and their work for the structural validations; the staff at the Dubochet Center for Imaging (DCI) in Lausanne for cryo-EM data collection and processing; SCITAS at EPFL for support in the computational simulations; the staff at GECF for assistance with deep sequencing and members of FCCS for assistance in FACS. We also thank Dr. Andrea Moretti from Malvern Panalytical for his support to run the Grating-Coupled Interferometry on Creoptix Wave and giving access to the instrument. We express our gratitude to Prof. Eva-Maria Strauss for providing *de novo* hyperstable proteins for our scaffold database. Finally, we thank Prof. Nicolas Thomä and Dr. Kelvin Lau for their feedback on the manuscript.

Funding

This work was supported the Swiss National Science Foundation grant 310030_197724 (B.E.C, A.M., M.E.), TMGC-3_213750 (B.E.C, S.B.), 200020_214843 (P.W.L., S.J.M.); the National Center of Competence in Research in Molecular Systems Engineering grant 182895 (B.E.C and A.M.); the National Center of Competence in Research in Catalysis grant 180544 (P.S.); EPSRC Turing AI World-Leading Research Fellowship No. EP/X040062/1 (M.B.); Microsoft Research AI4Science (B.E.C and A.S.); VantAI (R.M.N.); Huawei Technologies Düsseldorf (B.E.C, L.S.); Reprodivac grant SEFRI 22.00135 (B.E.C, E.E.); the H2020 Marie Sklodowska-Curie EPFL-Fellows grant (P.G.); the “Peter und Traudl Engelhorn Stiftung” (M.P.).

Author contributions

A.M., S.B. and A.S. contributed equally to this work. A.M. and B.E.C led the project. A.M., S.B., P.W.L. and M.E. performed the experimental work. A.M., S.B., M.P. and L.S. designed the experimental methodology. A.M. and A.S. performed the computational work and protein design. A.M., A.S., P.G., E.E. and R.M.N. contributed to the design of the computational pipeline. M.P. solved the crystal structure. L.R. synthesized the small molecule analogs. S.G. and J.S. participated in the expression and purification of proteins. P.S., S.J.M., M.B. and B.E.C provided supervision and acquired the necessary funding. A.M., S.B., A.S., M.P. and B.E.C wrote the manuscript with inputs from all authors.

bioRxiv preprint doi: https://doi.org/10.1101/2024.03.25.585721; this version posted March 28, 2024. The copyright holder for this preprint (which was not certified by peer review) is the author/funder, who has granted bioRxiv a license to display the preprint in perpetuity. It is made available under aCC-BY-NC-ND 4.0 International license.

Competing interest

Ecole Polytechnique Fédérale de Lausanne (EPFL) has filed a patent application that incorporates findings presented previously in *MaSIF-seed*. P.G., A.M., M.B. and B.E.C. are named as co-inventors on this patent (US Patent Office, US20230395187A1).

Data and material availability

Crystal structure of DBAct553_2 in complex with Actinonin-bound PDF1 has been deposited at the PDB under the accession code 8S1X (DOI: https://doi.org/10.2210/pdb8S1X/pdb). *MaSIF-neosurf* and the Rosetta design scripts are available on GitHub (https://github.com/LPDI-EPFL/masif-neosurf). The scaffold database generated for grafting the seed provided by *MaSIF-neosurf* is partly available at Zenodo (https://zenodo.org/records/7643697#.Y-z533ZKhaQ) and partly on Github (https://github.com/strauchlab/DBP and https://github.com/strauchlab/scaffold_design/). All other data needed to evaluate the conclusions in this paper are present either in the main text or the supplementary materials.

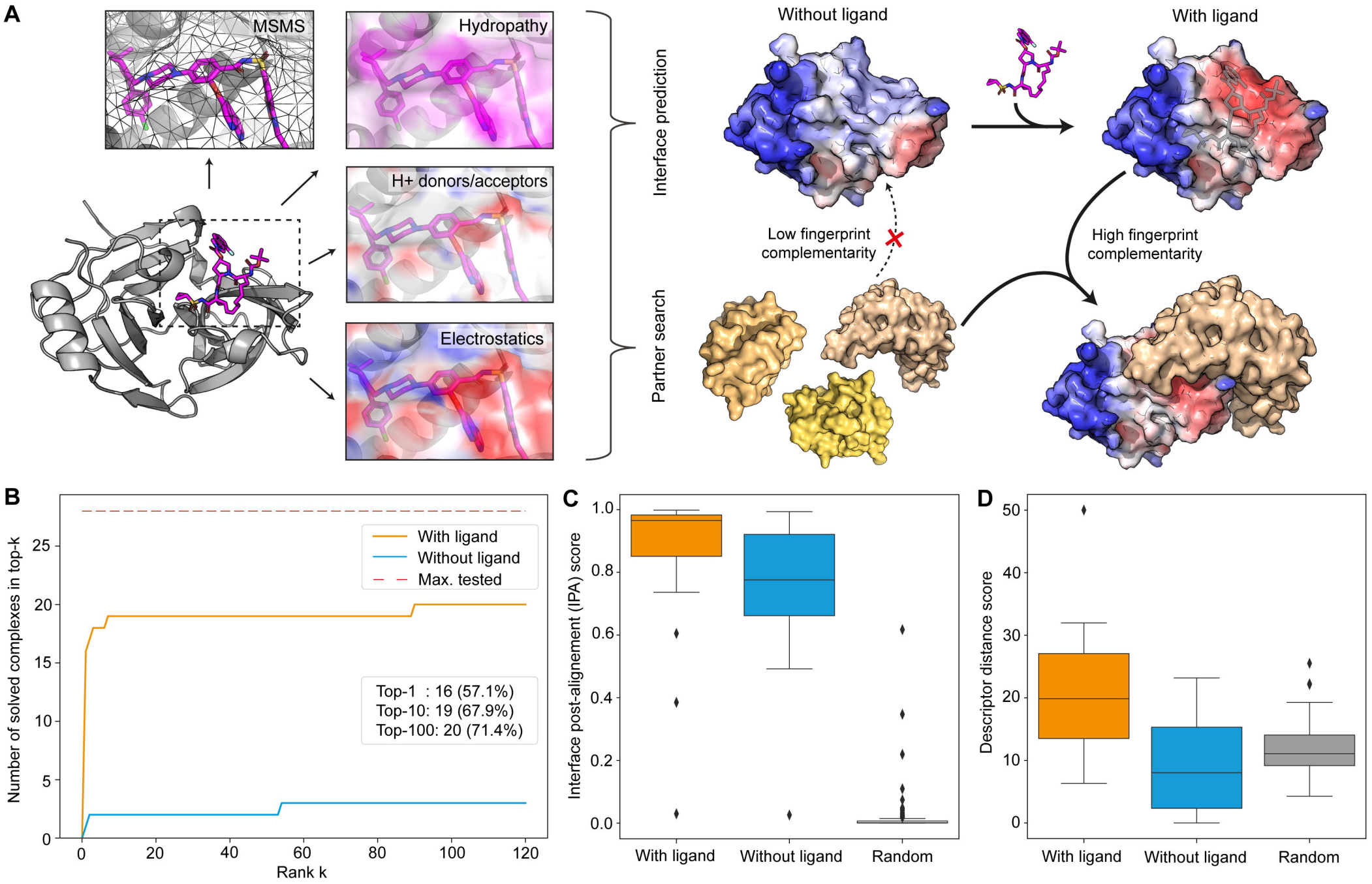
A
MSMS
Hydropathy
H+ donors/acceptors
Electrostatics
Interface prediction
Partner search
Without ligand
With ligand
Low fingerprint complementarity
High fingerprint complementarity
B
With ligand
Without ligand
Max. tested
Top-1 : 16 (57.1%)
Top-10: 19 (67.9%)
Top-100: 20 (71.4%)
Number of solved complexes in top-k
Rank k
C
Interface post-alignement (IPA) score
With ligand
Without ligand
Random
D
Descriptor distance score
With ligand
Without ligand
Random

(which was not certified by peer review) is the author/funder, who has granted bioRxiv a license to display the preprint in perpetuity. It is
made available under aCC-BY-NC-ND 4.0 International license.

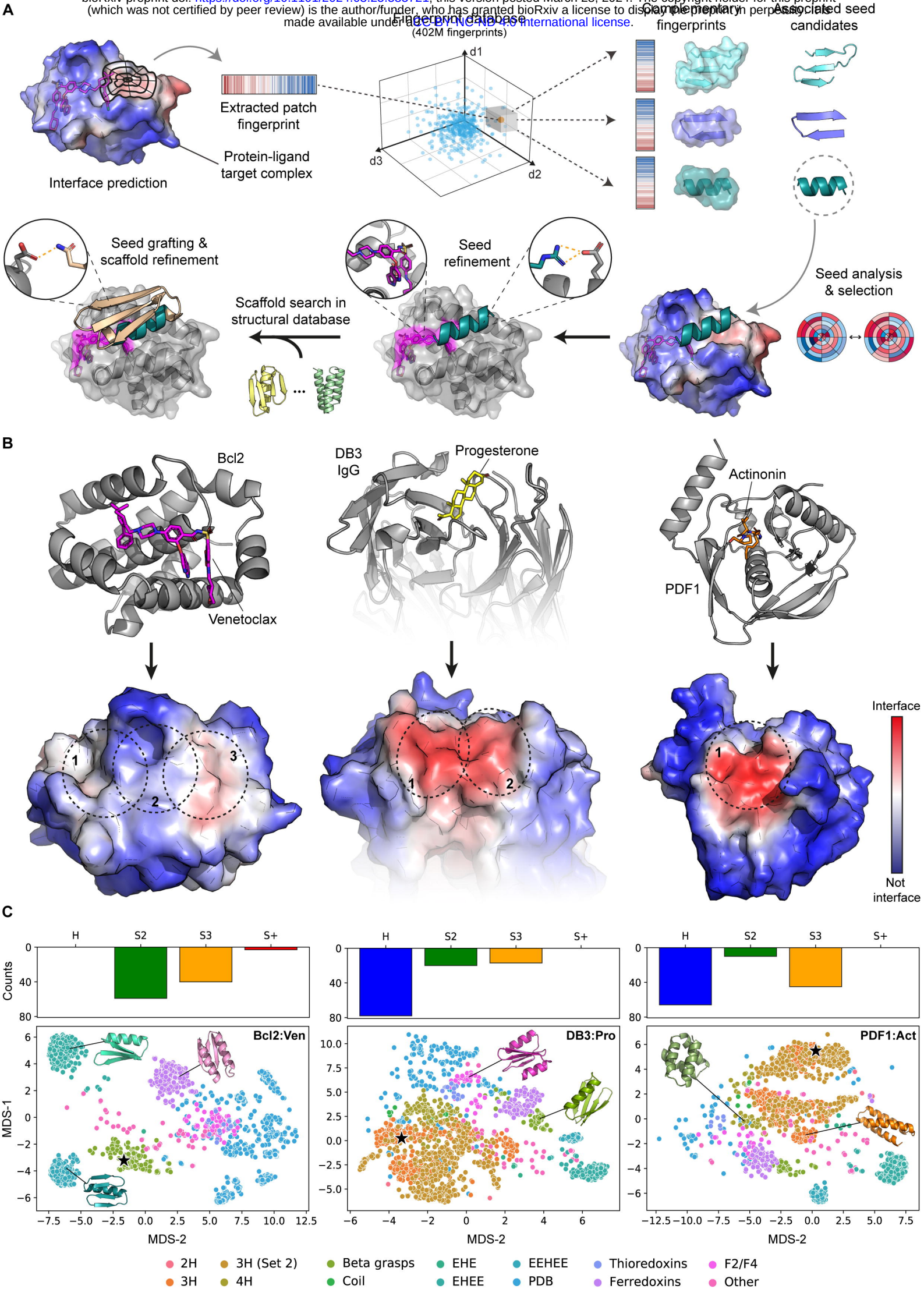

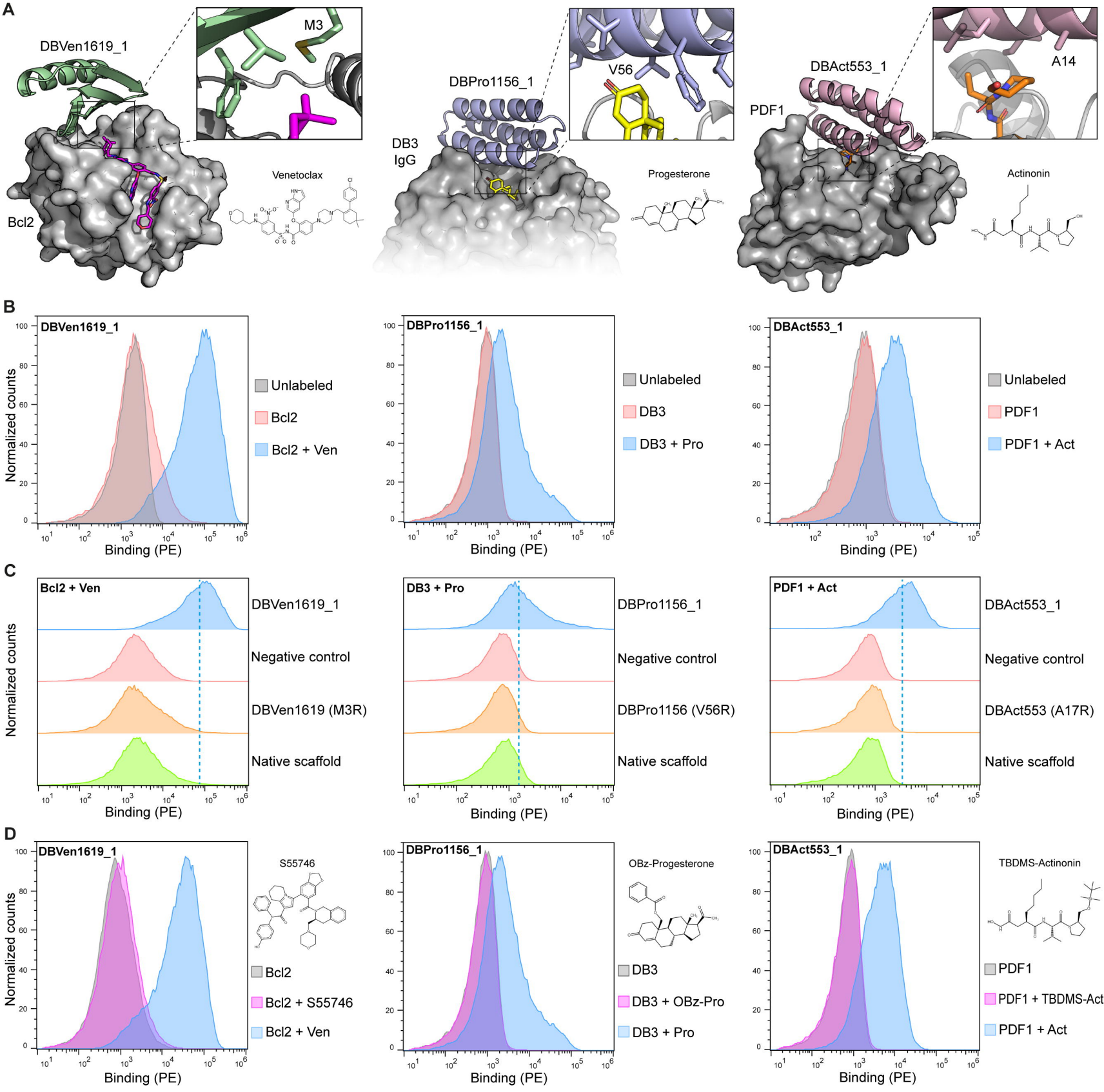
A
DBVen1619_1
M3
Bcl2
Venetoclax
DBPro1156_1
V56
DB3
IgG
Progesterone
DBAct553_1
A14
PDF1
Actinonin
B
DBVen1619_1
Unlabeled
Bcl2
Bcl2 + Ven
DBPro1156_1
Unlabeled
DB3
DB3 + Pro
DBAct553_1
Unlabeled
PDF1
PDF1 + Act
Normalized counts
Binding (PE)
C
Bcl2 + Ven
DBVen1619_1
Negative control
DBVen1619 (M3R)
Native scaffold
DB3 + Pro
DBPro1156_1
Negative control
DBPro1156 (V56R)
Native scaffold
PDF1 + Act
DBAct553_1
Negative control
DBAct553 (A17R)
Native scaffold
D
DBVen1619_1
S55746
Bcl2
Bcl2 + S55746
Bcl2 + Ven
DBPro1156_1
OBz-Progesterone
DB3
DB3 + OBz-Pro
DB3 + Pro
DBAct553_1
TBDMS-Actinonin
PDF1
PDF1 + TBDMS-Act
PDF1 + Act

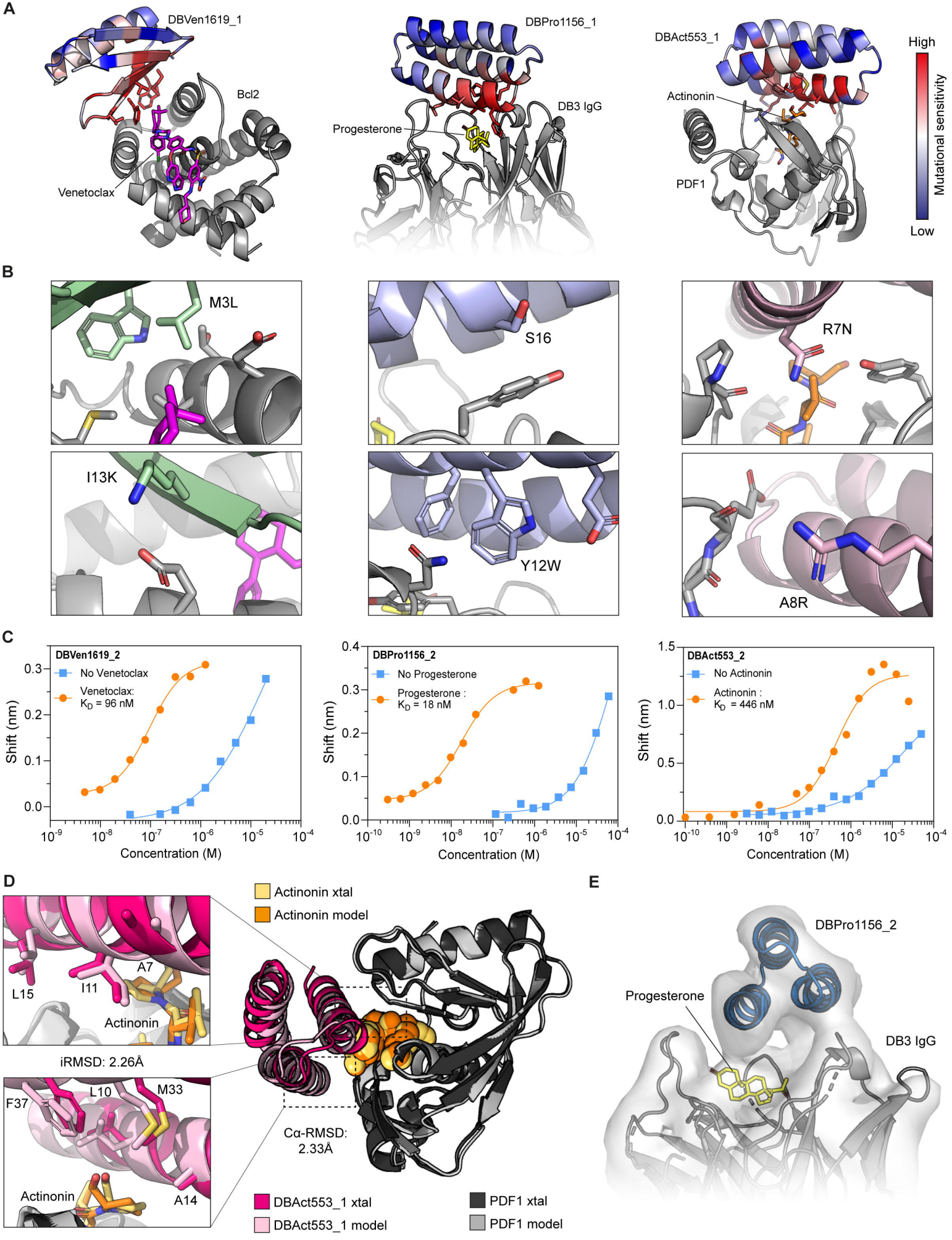
A
DBVen1619_1
Bcl2
Venetoclax
DBPro1156_1
DB3 IgG
Progesterone
DBAct553_1
Actinonin
PDF1
High
Mutational sensitivity
Low
B
M3L
S16
R7N
I13K
Y12W
A8R
C
DBVen1619_2
No Venetoclax
Venetoclax:
K_D = 96 nM
Shift (nm)
Concentration (M)
DBPro1156_2
No Progesterone
Progesterone :
K_D = 18 nM
DBAct553_2
No Actinonin
Actinonin :
K_D = 446 nM
D
Actinonin xtal
Actinonin model
L15
I11
A7
Actinonin
iRMSD: 2.26Å
F37
L10
M33
A14
Cα-RMSD:
2.33Å
DBAct553_1 xtal
DBAct553_1 model
PDF1 xtal
PDF1 model
E
DBPro1156_2
Progesterone
DB3 IgG

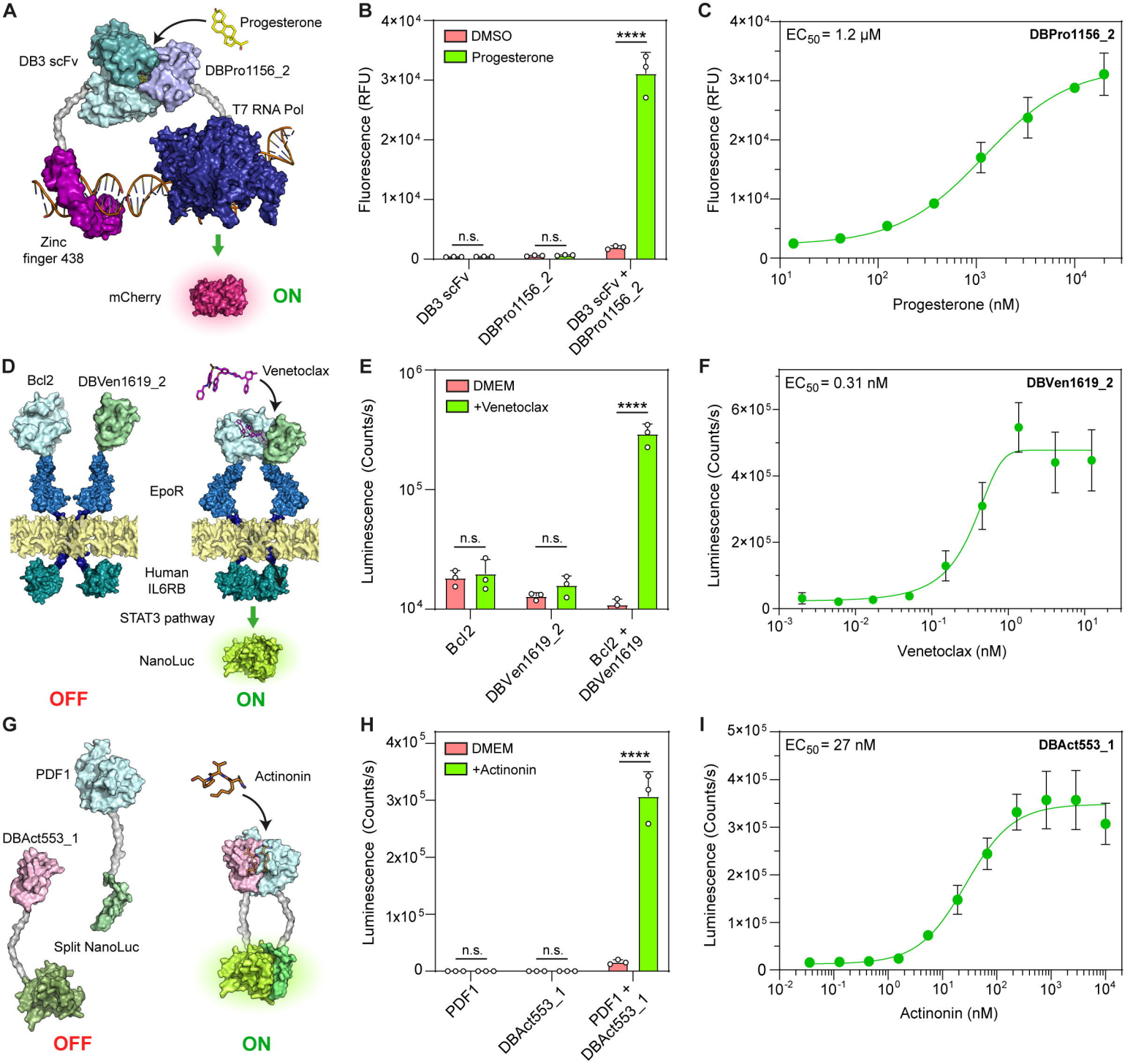
A
Progesterone
DB3 scFv
DBPro1156_2
T7 RNA Pol
Zinc
finger 438
mCherry
ON
B
DMSO
Progesterone
****
Fluorescence (RFU)
n.s.
n.s.
DB3 scFv
DBPro1156_2
DB3 scFv +
DBPro1156_2
C
EC50 = 1.2 µM
DBPro1156_2
Fluorescence (RFU)
Progesterone (nM)
D
Bcl2
DBVen1619_2
Venetoclax
EpoR
Human
IL6RB
STAT3 pathway
NanoLuc
OFF
ON
E
DMEM
+Venetoclax
****
Luminescence (Counts/s)
n.s.
n.s.
Bcl2
DBVen1619_2
Bcl2 +
DBVen1619
F
EC50 = 0.31 nM
DBVen1619_2
Luminescence (Counts/s)
Venetoclax (nM)
G
PDF1
Actinonin
DBAct553_1
Split NanoLuc
OFF
ON
H
DMEM
+Actinonin
****
Luminescence (Counts/s)
n.s.
n.s.
PDF1
DBAct553_1
PDF1 +
DBAct553_1
I
EC50 = 27 nM
DBAct553_1
Luminescence (Counts/s)
Actinonin (nM)